© 2014. Published by The Company of Biologists Ltd | Development (2014) 141, 2825-2837 doi:10.1242/dev.107409

RESEARCH ARTICLE

Essential role of the ERK/MAPK pathway in blood-placental barrier formation

Valérie Nadeau and Jean Charron*

ABSTRACT

The mammalian genome contains two ERK/MAP kinase kinase genes, *Map2k1* and *Map2k2*, which encode dual-specificity kinases responsible for ERK activation. Loss of *Map2k1* function in mouse causes embryonic lethality due to placental defects, whereas *Map2k2* mutants have a normal lifespan. The majority of *Map2k1*$^{+/-}$ *Map2k2*$^{+/-}$ embryos die during gestation from the underdevelopment of the placenta labyrinth, demonstrating that both kinases are involved in placenta formation. *Map2k1*$^{+/-}$ *Map2k2*$^{+/-}$ mutants show reduced vascularization of the labyrinth and defective formation of syncytiotrophoblast layer II (SynT-II) leading to the accumulation of multinucleated trophoblast giant cells (MTGs). To define the cell type-specific contribution of the ERK/MAPK pathway to placenta development, we performed deletions of *Map2k1* function in different *Map2k1 Map2k2* allelic backgrounds. Loss of MAP kinase kinase activity in pericytes or in allantois-derived tissues worsens the MTG phenotype. These results define the contribution of the ERK/MAPK pathway in specific embryonic and extraembryonic cell populations for normal placentation. Our data also indicate that MTGs could result from the aberrant fusion of SynT-I and -II. Using mouse genetics, we demonstrate that the normal development of SynT-I into a thin layer of multinucleated cells depends on the presence of SynT-II. Lastly, the combined mutations of *Map2k1* and *Map2k2* alter the expression of several genes involved in cell fate specification, cell fusion and cell polarity. Thus, appropriate ERK/MAPK signaling in defined cell types is required for the proper growth, differentiation and morphogenesis of the placenta.

KEY WORDS: MAP2K1 (MEK1), MAP2K2 (MEK2), Syncytiotrophoblast differentiation, Placenta morphogenesis

INTRODUCTION

The placenta is a transient organ that permits the mammalian embryo to survive in the uterine environment. The fetal blood vessels are closely juxtaposed to the maternal blood network, allowing efficient gas and nutrient exchange and evacuation of fetal wastes. The separation between the fetal and maternal blood circulations is crucial for the immune tolerance of the mother to embryo antigens to allow normal embryonic development throughout gestation (Rossant and Cross, 2001). In mice, placenta formation initiates around embryonic day (E) 8.5 with the fusion of the chorion with the allantois to produce the labyrinthine region. The chorion gives rise to trophoblasts, whereas endothelial cells and pericytes originate from the allantois. As the labyrinth develops, the chorionic ectoderm undergoes extensive branching morphogenesis and vascularization to form a highly branched villous structure that provides the surface required for the maternal-fetal exchanges. The trophoblasts play a structural role and participate in the vascularization of the placenta. Thus, both extraembryonic and embryonic tissues cooperate in placenta formation.

Establishment of the blood-placental barrier between maternal and fetal circulations is crucial for proper embryonic development. It is formed of fetal vascular endothelial cells and three types of trophoblast cells. A single fenestrated layer of sinusoidal trophoblast giant cells (S-TGCs) close to the maternal blood sinuses is juxtaposed to a double layer of syncytiotrophoblast (SynT) cells: SynT layer I (SynT-I) and layer II (SynT-II). The former lines maternal sinuses, whereas the latter is adjacent to fetal blood vessels (see Fig. 8) (Simmons et al., 2008). Each SynT layer forms, by cell fusion, a postmitotic multinucleated syncytium that fulfills transport functions. The SynT layers guarantee isolation between the maternal and embryonic blood circulations by reducing the number of intercellular junctions. Thus, maternal and fetal blood cells are isolated by a tight, triple cell layer comprising SynT-I and -II and the fetal vascular endothelial cells.

Cell fusion is a highly controlled process that entails fusogenic proteins inducing membrane fusion (Palfreyman and Jorgensen, 2009). In placenta, syncytins A and B are two fusogenic proteins encoded by the retrovirus-derived genes *Syna* and *Synb* (Dupressoir et al., 2005). They are implicated in trophoblast cell fusion to form SynT-I and -II, respectively (Dupressoir et al., 2009, 2011). Differentiation of SynT-II cells is also coupled to the expression of *Gcm1*, an early marker of SynT-II that encodes a transcriptional regulator of *Synb* (Anson-Cartwright et al., 2000; Simmons et al., 2008).

To facilitate maternal-fetal exchanges, both SynT layers express specific transporters that show polarized localization. In murine placenta, the glucose transporters GLUT1 (SLC2A1) and GLUT3 (SLC2A3) are localized at the apical membrane of SynT-I, and GLUT1 is also present at the basal membrane of SynT-II (Shin et al., 1997, 1996). The monocarboxylate transporters of lactate MCT1 (SLC16A1) and MCT4 (SLC16A3) are located at the SynT-I apical and SynT-II basal membranes, respectively (Nagai et al., 2010). Thus, SynT cells are highly polarized to accomplish their role as an epithelial barrier.

As revealed by the characterization of mutant mouse lines, anomalies in SynT cell fusion and cell polarity affect placenta morphogenesis, impairing maternal-fetal exchanges, contributing to growth retardation and ultimately causing embryonic death (Anson-Cartwright et al., 2000; Dupressoir et al., 2009, 2011; Sripathy et al., 2011). For instance, the placenta of mice mutant for genes involved in the ERK/MAPK pathway exhibits defects associated with an accumulation of MTGs (Galabova-Kovacs et al., 2006; Kubota et al., 1999; Nadeau et al., 2009; Parekh et al., 2004; Qian et al., 2000). In *Map2k1*$^{+/-}$ *Map2k2*$^{+/-}$ mutants, cell lineage analysis showed that

Centre de recherche sur le cancer de l'Université Laval, Centre Hospitalier Universitaire de Québec, L'Hôtel-Dieu de Québec, 9 rue McMahon, Québec, QC, Canada G1R 2J6.

*Author for correspondence (jean.charron@crhdq.ulaval.ca)

Received 19 December 2013; Accepted 13 May 2014

Development (2014) 141, 2825-2837 doi:10.1242/dev.107409

MTGs are derived from SynT-II (Nadeau et al., 2009). Moreover, the specific ablation of one *Map2k1* allele in SynT-II with *Gcm1Cre* mice in a *Map2k2*$^{+/-}$ background (*Map2k1*$^{+/flox}$ *Map2k2*$^{+/-}$ *Tg*$^{+/Gcm1Cre}$) caused MTG formation, revealing the cell-autonomous function of *Map2k1* in SynT-II. However, the presence of a *Map2k2* mutant allele in all cell types does not exclude the possibility that the ERK/MAPK pathway may be necessary in other cell types for placenta integrity. Mice mutant for the grainyhead transcription factor LBP-1a (UBP1), a target of ERK, also present an accumulation of MTG-like structures referred to as 'amorphous material' (Pagon et al., 2003; Parekh et al., 2004; Volker et al., 1997). This MTG-like phenotype cannot be rescued in tetraploid complementation assays, indicating that the defect is non-cell-autonomous and secondary to a defective allantoic mesoderm. The allantoic mesoderm is known to provide signals to the chorionic ectoderm to initiate placenta morphogenesis and SynT-II differentiation (Hemberger and Cross, 2001).

To define the contribution of *Map2k1* and *Map2k2* in extraembryonic- and embryonic-derived placental cell types, we generated a series of *Map2k1 Map2k2* compound allelic mutants using the *Map2k1* conditional allele and distinct *Cre* mouse lines. The specific ablation of *Map2k1* function in pericytes or in allantois-derived tissues aggravated the MTG placenta phenotype compared with *Map2k1*$^{+/-}$ *Map2k2*$^{+/-}$ specimens, demonstrating the importance of the ERK/MAPK pathway in defined embryonic and extraembryonic cell types for correct placenta development. Characterization of the MTGs indicated that they expressed markers of both SynT-I and -II. Mechanistically, loss of ERK/MAPK activity in SynT cells led to decreased expression of GCM1 and PPARγ, which are known to be essential for proper placental development (Anson-Cartwright et al., 2000; Barak et al., 1999). Additionally, the SynT-I apical proteins MCT1, GLUT1 and atypical protein kinase C zeta (PKCζ) were mislocalized. Attenuation of the ERK/MAPK pathway in SynT-II, pericytes and endothelial cells by genetic means thus perturbs the normal SynT cell fusion process, thus contributing to MTG formation and causing embryonic death.

RESULTS

Map2k1 gene deletion in SynT-II does not compromise embryo survival or placenta development

We showed that placenta from *Map2k1*$^{+/flox}$ *Map2k2*$^{+/-}$ *Tg*$^{+/Gcm1Cre}$ conceptuses contains MTGs, indicating the cell-autonomous function of *Map2k1* in SynT-II in a *Map2k2*$^{+/-}$ background (Table 1) (Nadeau et al., 2009). To test the role of *Map2k1* in SynT-II differentiation and MTG formation, both *Map2k1* alleles were deleted in SynT-II using the *Gcm1Cre* mouse line. *Map2k1*$^{flox/-}$ *Rosa*$^{+/lacZ}$ *Tg*$^{+/Gcm1Cre}$ mice were viable, indicating that the loss of *Map2k1* function in SynT-II is not essential for placenta formation. Placenta from *Map2k1*$^{flox/-}$ *Rosa*$^{+/lacZ}$ *Tg*$^{+/Gcm1Cre}$ mutants was similar to that of controls (supplementary material Fig. S2A,D). As shown by X-Gal staining, the *Rosa*^{lacZ} *Cre* reporter allele was activated in SynT-II (supplementary material Fig. S2E). No MAP2K1 immunostaining was detected in mutants, confirming efficient deletion of the *Map2k1*^{flox} allele (supplementary material Fig. S2B,C). Few MTGs were observed in *Map2k1*$^{flox/-}$ *Rosa*$^{+/lacZ}$ *Tg*$^{+/Gcm1Cre}$ placentas but they were comparable in size and number to those detected in *Map2k2*$^{-/-}$ placentas (supplementary material Fig. S2D; Table 1). Thus, the lack of *Map2k1* function in SynT-II can cause MTG formation but at a low penetrance and expressivity that does not compromise embryo survival.

A defective allantoic mesoderm can contribute to the formation of MTG-like structures, as shown in *Lbp-1a* mutant mice (Parekh et al., 2004). The MTGs present in *Map2k1*$^{+/-}$ *Map2k2*$^{+/-}$ specimens were mainly located near the junction with the allantoic mesoderm (69.4%; Fig. 1) (Nadeau et al., 2009). ERK modulates LBP-1a activity, leading us to hypothesize that the loss of one *Map2k1* allele in allantoic mesoderm combined with the *Map2k1* mutation in SynT-II can worsen the MTG phenotype. This was assessed by generating *Map2k1*$^{flox/-}$ *Rosa*$^{+/lacZ}$ *Tg*$^{+/Gcm1Cre}$ *Tg*$^{+/Sox2Cre}$ specimens. The loss of *Map2k1* function in SynT-II and allantois-derived cells resulted in an increase in the number and size of MTGs, indicating a tendency toward an aggravated MTG phenotype compared with *Map2k1*$^{flox/-}$ *Tg*$^{+/Gcm1Cre}$ specimens (P=0.38 and P=0.42, respectively; supplementary material Fig. S2G; Table 1).

Table 1. MTG phenotype in the various *Map2k1 Map2k2* mutants

Genotype	Number of specimens with MTGs*	Number of MTGs per specimen‡	Surface occupied by MTGs (×10^{-3} mm^2)	Survival at birth (%)
Map2k1$^{flox/-}$ *Tg*$^{+/Sox2Cre}$	1/5	0.2±0.4	0.6±1.3	100
Map21$^{+/flox}$ *Map2k2*$^{+/-}$ *Tg*$^{+/Sox2Cre}$	1/9	0.1±0.3	2.2±6.5	100
Map2k1$^{+/-}$	3/13	0.7±1.3	3.2±6.7	100
Map2k2$^{-/-}$	3/7	1.4±1.9	11.1±17.7	100
Map2k1$^{flox/-}$ *Tg*$^{+/Gcm1Cre}$	7/10	2.1±2.8	20.4±19.8	100
Map2k1$^{+/flox}$ *Map2k2*$^{+/-}$ *Tg*$^{+/Gcm1Cre}$	5/7	3.1±2.5	31.3±48.4	n.d.
Map2k1$^{flox/-}$ *Tg*$^{+/Gcm1Cre}$ *Tg*$^{+/Sox2Cre}$	3/4	5.0±5.6	41.7±45.0	n.d.
Map2k1$^{+/-}$ *Map2k2*$^{+/-}$	13/13	8.3±4.3	89.7±50.1	10
Map2k1$^{flox/-}$ *Map2k2*$^{+/-}$ *Tg*$^{+/Gcm1Cre}$	7/8	10.4±6.8	103.7±78.0	n.d.
Map2k1$^{flox/-}$ *Map2k2*$^{+/-}$ *Dermo1*$^{+/Cre}$	11/11	13.3±3.6	102.7±30.6	n.d.
Map2k1$^{flox/-}$ *Map2k2*$^{+/-}$ *Tg*$^{+/Sox2Cre}$	20/20	17.7±6.8	133.0±64.8	n.d.

*The number of specimens with MTGs out of the total number of specimens analyzed at E12.5.

‡Four sections ~100 μm apart were analyzed for each specimen to estimate the number of MTGs.

Values are mean±s.d.

n.d., not determined.

P-values in text refer to Student's *t*-test analyses between the genotypes indicated. The number of specimens used per genotype is indicated.

Contribution of ERK/MAPK signaling in allantois-derived tissues for SynT-II differentiation

To characterize the placenta phenotype of *Map2k1*$^{+/flox}$ *Map2k2*$^{+/-}$ *Tg*$^{+/Gcm1Cre}$ specimens, we evaluated the number and size of MTGs. Compared with *Map2k1*$^{+/-}$ *Map2k2*$^{+/-}$ specimens, labyrinth growth was less affected and the number and the area occupied by MTGs were significantly reduced (P=0.027 and P=0.025, respectively; Fig. 1C, Table 1). The remaining *Map2k1* allele was inactivated in SynT-II by generating *Map2k1*$^{flox/-}$ *Map2k2*$^{+/-}$ *Tg*$^{+/Gcm1Cre}$ specimens. The number and the size of MTGs were statistically increased compared with *Map2k1*$^{+/flox}$ *Map2k2*$^{+/-}$ *Tg*$^{+/Gcm1Cre}$ specimens (P=0.03 and P=0.049, respectively) and comparable to the *Map2k1*$^{+/-}$ *Map2k2*$^{+/-}$ phenotype (Fig. 1B-D, Table 1). *Map2k1* deletion in cell types other than SynT-II cells combined with reduced *Map2k2* function is thus required for full penetrance and expressivity of the MTG phenotype.

To analyze whether reduced ERK/MAPK signaling in allantoic mesoderm contributes to MTG formation, we generated *Map2k1*$^{+/flox}$ *Map2k2*$^{+/-}$ *Tg*$^{+/Sox2Cre}$ conceptuses in which one *Map2k1* allele was mutated in allantois. One out of nine specimens analyzed presented

Development (2014) 141, 2825-2837 doi:10.1242/dev.107409

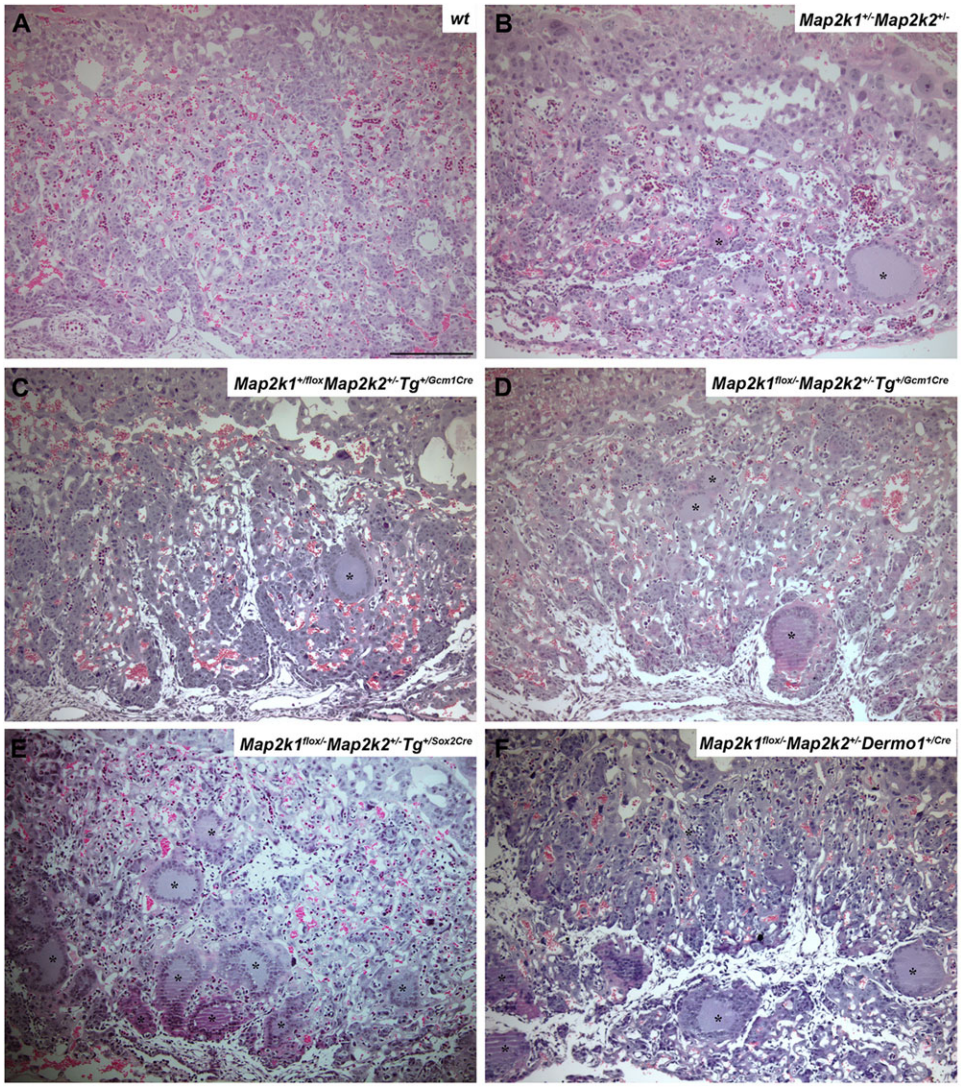

Fig. 1. Placenta phenotypes in *Map2k1 Map2k2* allelic series generated by Cre-mediated recombination. H&E staining was performed on placenta sections from E12.5 mouse embryos carrying different combinations of *Map2k1 Map2k2* mutations, as indicated. MTGs are identified by asterisks. Scale bar: 200 μm.

a placental phenotype, indicating that deletion of one *Map2k1* allele in allantois-derived tissues in a *Map2k2*$^{+/-}$ background was insufficient for MTG formation (Table 1). In *Map2k1*$^{flox/-}$ *Map2k2*$^{+/-}$ *Tg*$^{+/Sox2Cre}$ specimens, in which both *Map2k1* alleles were deleted in allantois-derived tissues in a *Map2k1*$^{+/-}$ *Map2k2*$^{+/-}$ background, the placenta phenotype was exacerbated, with more MTGs ($P=3\times10^{-5}$) occupying an increased placental area ($P=0.04$) when compared with *Map2k1*$^{+/-}$ *Map2k2*$^{+/-}$ specimens (Fig. 1E, Table 1). These results highlight the importance of *Map2k1* function in allantois-derived tissues during SynT-II differentiation.

The *Sox2Cre*-mediated recombination occurs in all allantois-derived cell types, including endothelial cells and pericytes. In the labyrinth, SynT-II is flanked by pericytes and embryonic vascular endothelial cells (supplementary material Fig. S1) (Hayashi et al., 2002). The role of ERK/MAPK signaling in pericytes was tested with *Dermo1Cre* mice, which drive deletion in pericytes of the placenta (supplementary material Fig. S1). *Map2k1*$^{flox/-}$ *Map2k2*$^{+/-}$ *Dermo1*$^{+/Cre}$ specimens, in which both *Map2k1* alleles were deleted in pericytes in a *Map2k1*$^{+/-}$ *Map2k2*$^{+/-}$ background, were produced. Placentas displayed more MTGs than *Map2k1*$^{+/-}$ *Map2k2*$^{+/-}$ specimens ($P=0.006$), with no difference in size ($P=0.45$; Table 1). However, the phenotype was not as severe as that seen in *Map2k1*$^{flox/-}$ *Map2k2*$^{+/-}$ *Tg*$^{+/Sox2Cre}$ specimens; fewer MTGs were observed and the area they occupied was reduced ($P=0.02$ and $P=0.09$, respectively; Fig. 1E,F, Table 1). Therefore, the placenta phenotype from *Map2k1*$^{flox/-}$ *Map2k2*$^{+/-}$ *Dermo1*$^{+/Cre}$ embryos did not fully recapitulate the *Map2k1*$^{flox/-}$ *Map2k2*$^{+/-}$ *Tg*$^{+/Sox2Cre}$ phenotype. These results suggest that, even though pericytes are involved in SynT-II differentiation, they are not the sole allantois-derived cell type requiring the ERK/MAPK pathway for placenta formation. Thus, proper expression levels of *Map2k1* and *Map2k2* are essential in allantois and extraembryonic tissues to support SynT-II formation and differentiation.

MTGs have a double identity

In vivo cell lineage experiments demonstrated that MTGs in *Map2k1*$^{+/-}$ *Map2k2*$^{+/-}$ placentas derive from SynT-II (Nadeau et al., 2009). However, expression of *Gcm1*, a SynT-II marker, was not observed in MTGs. To define the origin of the MTGs, staining with specific SynT-I and SynT-II markers was performed. Oil Red O staining, which labels lipid droplets present in SynT-II, was observed in MTGs (Fig. 2A,B) (Barak et al., 1999). CEBPα and *Synb* expression, both markers of SynT-II, was detected in SynT-II in wild-type (wt) and *Map2k1*$^{+/-}$ *Map2k2*$^{+/-}$ placenta, but not in MTGs (Fig. 2C-F) (Simmons et al., 2008). By contrast, MTGs were positive for *Syna* expression, a SynT-I marker

Development (2014) 141, 2825-2837 doi:10.1242/dev.107409

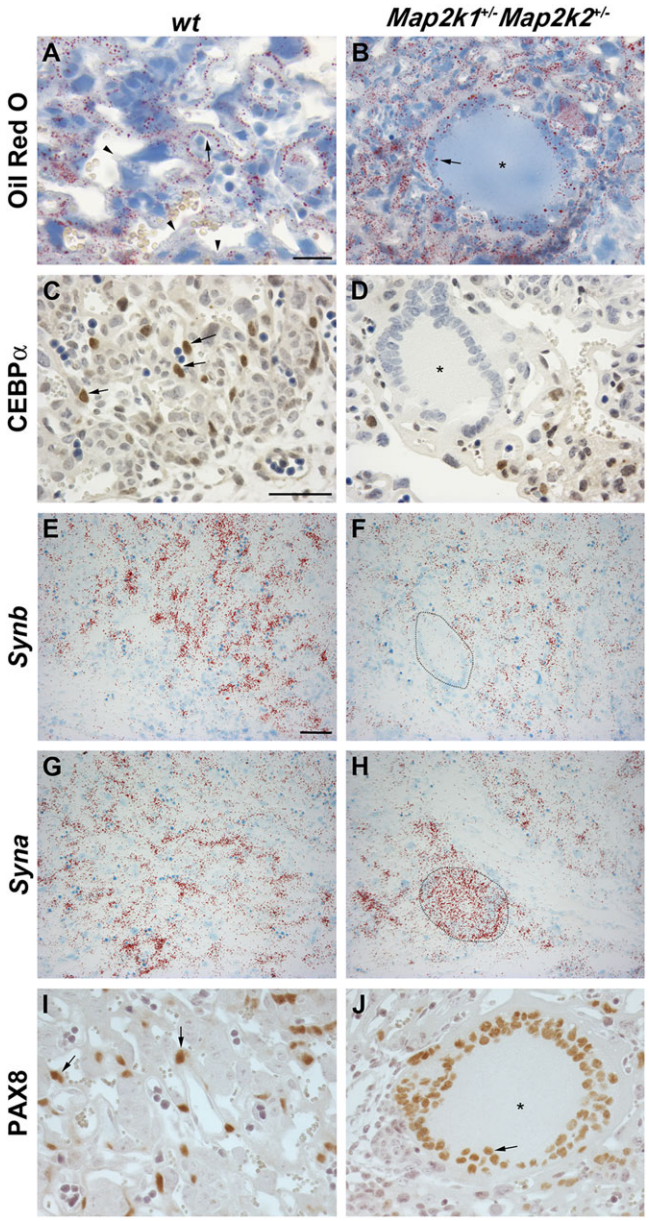

Fig. 2. Characterization of MTGs in placenta from E12.5 *Map2k1*$^{+/-}$ *Map2k2*$^{+/-}$ embryos. (A) Oil Red O staining revealed the presence of lipid droplets in SynT-II (arrows) but not in SynT-I (arrowheads) in placenta from an E12.5 wt embryo. (B) In *Map2k1*$^{+/-}$ *Map2k2*$^{+/-}$ specimens, the presence of lipid droplets (arrow) was observed in MTGs (asterisk). (C,D) CEBPα immunostaining labeled the nuclei of SynT-II cells in wt (C, arrows) and *Map2k1*$^{+/-}$ *Map2k2*$^{+/-}$ (D) specimens. No signal was observed in MTG nuclei. (E-H) Expression of *Synb* (E,F) and *Syna* (G,H), which are markers of SynT-II and SynT-I, respectively, was revealed by ISH. MTGs expressed *Syna* but not *Synb* (MTG encircled). (I,J) PAX8 expression was detected by IHC in SynT-I and in the nuclei of MTGs (arrows). Scale bars: 20 μm in A,B; 50 μm in C-J.

(Fig. 2G,H). Altogether, these data suggest that MTGs possess a double identity.

To validate the SynT-I identity of MTGs, we looked for additional SynT-I markers. The transcription factor PAX8 is expressed in mouse and human placenta. Its expression is increased by cAMP, a pathway involved in SynT fusion (Chang et al., 2005; Ferretti et al., 2005; Ohno et al., 1999; Wice et al., 1990). PAX8 expression was detected in SynT-I nuclei (Fig. 2I). This was confirmed by co-labeling experiments with MCT1, a marker of the apical membrane of SynT-I (supplementary material Fig. S3A). We also took advantage of the EGFP expression in *Rosa*$^{+/\text{Tomato-EGFP}}$ *Tg*$^{+/\text{Gcm1Cre}}$ placenta combined with PAX8 immunodetection. EGFP labeled both apical and basal SynT-II membranes. No PAX8-positive nuclei were surrounded by EGFP-labeled membranes, demonstrating that PAX8 was not expressed in SynT-II. Moreover, EGFP-labeled SynT-II membranes were localized between PAX8-positive nuclei and fetal blood cells (supplementary material Fig. S3B). Thus, PAX8 appears to be a new SynT-I cell marker (supplementary material Fig. S3C). In *Map2k1*$^{+/-}$ *Map2k2*$^{+/-}$ placenta, nuclear PAX8 staining was observed in MTGs, indicating that they display SynT-I characteristics (Fig. 2J).

We examined whether MTG formation could result from the fusion of both SynT layers. This was tested by immunostaining on adjacent sections of wt, *Map2k1*$^{+/-}$ *Map2k2*$^{+/-}$ and *Map2k1*$^{\text{flox}/-}$ *Map2k2*$^{+/-}$ *Tg*$^{+/\text{Sox2Cre}}$ specimens for the MCT1 and MCT4 markers, the latter being specific to SynT-II basal membrane. In controls, MCT1 was expressed in SynT-I (Fig. 3B), whereas MCT4 was detected in SynT-II (Fig. 3A). In *Map2k1*$^{+/-}$ *Map2k2*$^{+/-}$ and *Map2k1*$^{\text{flox}/-}$ *Map2k2*$^{+/-}$ *Tg*$^{+/\text{Sox2Cre}}$ placentas, MCT1 and MCT4 were co-expressed in MTGs, suggesting that MTGs were composed of both cell types (Fig. 3C-F). This was validated by MCT1 and MCT4 co-immunofluorescence staining. Most of the MTGs analyzed (18 out of 20) were positive for both markers (Fig. 3G-J). In a few cases, co-expression of MCT1 and MCT4 occurred along the entire MTG membrane (supplementary material Fig. S4). Thus, MTGs might result from the aberrant fusion of SynT-I and SynT-II layers.

SynT protein mislocalization in MTGs

The localization of syncytin and transporter proteins at the SynT membrane is crucial for the fusogenic and transport functions of SynT layers. Immunostaining showed MCT1 mislocalization in MTGs, as MCT1 staining became cytoplasmic in SynT-I adjacent to MTGs (Fig. 3D,F,I). Moreover, MTGs were large and round instead of adopting the characteristic elongated, thin shape of SynT. These observations prompted us to investigate whether other SynT proteins were mislocalized in MTGs. Abnormal expression of GLUT1, a glucose transporter located at the SynT-I apical and SynT-II basal membranes, was detected in MTG cytoplasm (Fig. 4A,B). We also analyzed the expression of connexin 26 (also known as GJβ2), which is found at the SynT-I basal and SynT-II apical membranes and contributes to gap junction formation (Shin et al., 1996). In MTGs, connexin 26 was correctly maintained at the membranes (Fig. 4C,D). Finally, we looked at the expression of PKCζ, a member of the apical complex necessary for epithelial cell polarity (McCaffrey and Macara, 2009). In controls, PKCζ staining was restricted to the apical domain of SynT-I cytoplasm. In mutants, PKCζ was detected throughout the MTG cytoplasm (Fig. 4E,F; supplementary material Fig. S5). The delocalization of MCT1 and PKCζ proteins was also observed in MTGs present in *Map2k1*$^{+/\text{flox}}$ *Map2k2*$^{+/-}$ *Tg*$^{+/\text{Gcm1Cre}}$ placenta (not shown). These results suggest that a reduction of ERK/MAPK signaling in SynT-II might be sufficient to perturb SynT-I and SynT-II integrity and to induce interlayer fusion and MTG formation.

Cellular ablation of SynT-II prevents SynT-I fusion

Electron microscopy data suggest that interactions of SynT-I cells with SynT-II are required to induce the formation of SynT-I

Development (2014) 141, 2825-2837 doi:10.1242/dev.107409

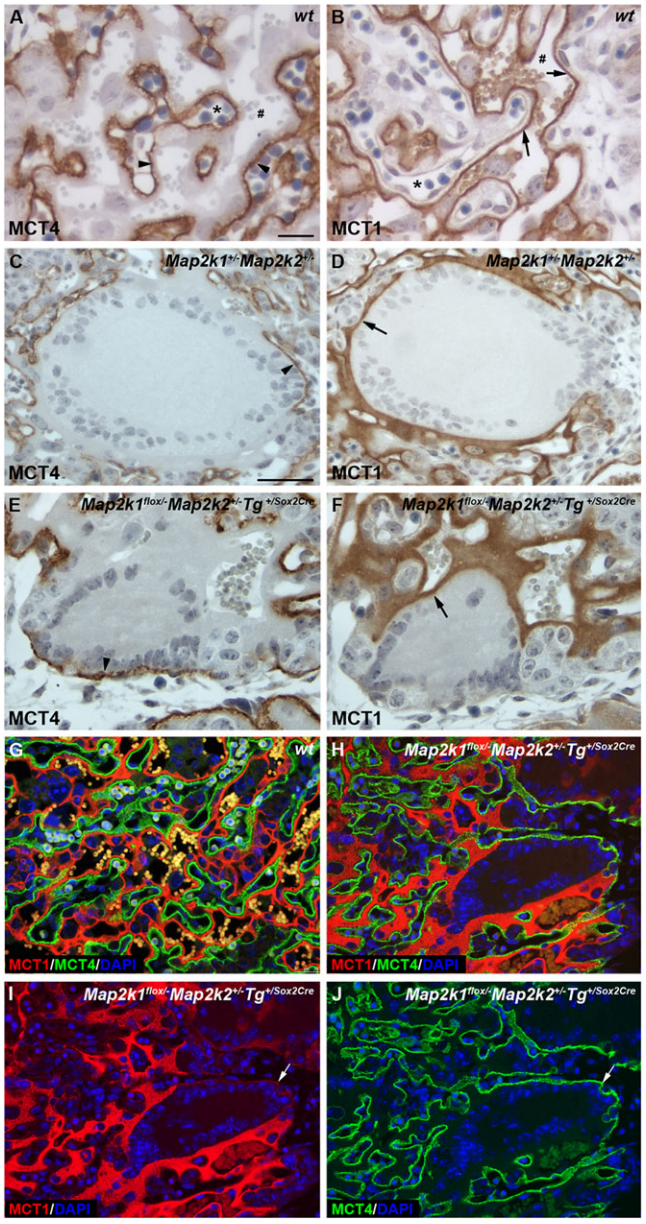

Fig. 3. MTGs express markers characteristic of SynT-I and SynT-II cells. (A-F) Expression of the membrane monocarboxylate transporters MCT1 (B,D,F) and MCT4 (A,C,E), which are specific markers of the SynT-I and SynT-II layers, respectively, was detected by IHC on adjacent sections of placenta from E12.5 wt (A,B), *Map2k1*$^{+/-}$ *Map2k2*$^{+/-}$ (C,D) and *Map2k1*$^{flox/-}$ *Map2k2*$^{+/-}$ *Tg*$^{+/Sox2Cre}$ (E,F) embryos. In wt specimens, MCT1 labeled SynT-I cells (B, arrows) lining the maternal blood sinuses (#), whereas MCT4 stained SynT-II cells (A, arrowheads) lining the fetal blood vessels (asterisk). MTGs stained positive for both MCT1 and MCT4 (C-F). (G,H) Co-localization of MCT1 and MCT4 proteins in MTGs was confirmed by IF on placenta sections from E12.5 wt (G) and *Map2k1*$^{flox/-}$ *Map2k2*$^{+/-}$ *Tg*$^{+/Sox2Cre}$ (H-J) embryos. In wt specimens, no co-localization was observed. In *Map2k1*$^{flox/-}$ *Map2k2*$^{+/-}$ *Tg*$^{+/Sox2Cre}$ placenta, MTGs were positive for both MCT1 and MCT4 (H). (I,J) Single channels of panel H for MCT1 (I) and MCT4 (J) are presented to show membrane co-labeling (arrows). Scale bars: 20 μm in A,B,E,F; 25 μm in G-J; 50 μm in C,D.

(Hernandez-Verdun, 1974). This is further supported by the lack of SynT-I in the placenta from *Gcm1* mutants, in which SynT-II is not produced (Anson-Cartwright et al., 2000). Our results suggested that inappropriate cell fusion between SynT-I and SynT-II might underlie MTG formation in *Map2k1 Map2k2* mutants, further indicating that cell-cell interactions between these two layers are important. To assess the relationship between the two SynT layers, a cellular ablation experiment was performed with the conditional diphteria toxin fragment A (DTA) allele (*Rosa*^{DTA}; Ivanova et al., 2005). Using *Gcm1Cre* mice, we specifically eliminated SynT-II upon DTA action during gestation. Conceptuses from *Rosa*$^{+/DTA}$ mice bred with *Tg*$^{+/Gcm1Cre}$ mice were recovered at E10.5, when labyrinth formation initiates and SynT-II functions are required. *Rosa*$^{+/DTA}$ *Tg*$^{+/Gcm1Cre}$ embryos were under-represented and their placenta had a more compact and less vascularized labyrinth compared with controls (supplementary material Table S3; Fig. 5). Embryonic vessels did not invade the labyrinth, supporting a role for SynT-II in migration guidance of endothelial cells. Rare maternal sinuses were visible but they did not penetrate efficiently into the labyrinth (Fig. 5C). To monitor the impact on the formation of SynT-I, co-labeling experiments with MCT1 and MCT4 were performed. In *Rosa*$^{+/DTA}$ *Tg*$^{+/Gcm1Cre}$ specimens, scarce MCT4-positive cells were detected showing the extent of the SynT-II deletion (Fig. 5G,H). MCT1 staining was observed in control and *Rosa*$^{+/DTA}$ *Tg*$^{+/Gcm1Cre}$ specimens. However, in *Rosa*$^{+/DTA}$ *Tg*$^{+/Gcm1Cre}$ placenta, MCT1 staining was associated with uninucleated cells (Fig. 5G,H). Thus, the cellular ablation of SynT-II perturbed the SynT-I cell fusion process, reflecting a dependence of SynT-I cells on SynT-II for their correct differentiation, confirming the original hypothesis.

Molecular repercussions of ERK/MAPK pathway dysregulation in the labyrinth

The ERK/MAPK pathway is known to regulate gene expression programs through the activation of transcription factors. To identify the downstream effectors of the ERK/MAPK cascade that could contribute to the MTG phenotype, we proceeded by a gene candidate approach. PPARγ, a known target of the ERK/MAPK cascade, is involved in SynT cell differentiation via the regulation of *Gcm1* (Burgermeister et al., 2007; Parast et al., 2009; Prusty et al., 2002). Loss of *Pparg* function causes embryonic lethality at mid-gestation due to trophoblast differentiation defects affecting syncytium formation (Barak et al., 1999). MTGs are also found in *Pparg*$^{-/-}$ placentas (Kubota et al., 1999). PPARγ and GCM1 immunodetection was performed on placenta from *Map2k1*$^{+/-}$ *Map2k2*$^{+/-}$ and *Map2k1*$^{flox/-}$ *Map2k2*$^{+/-}$ *Tg*$^{+/Sox2Cre}$ mutants. In controls, PPARγ expression was present in spongiotrophoblasts and in trophoblasts from the labyrinthine region. However, in mutants, PPARγ expression was reduced in the labyrinth trophoblasts and not detected in MTGs (Fig. 6A-D; not shown). Similarly, GCM1 expression was decreased in SynT-II of mutants and absent in MTGs (Fig. 6E-H). Thus, the loss of ERK/MAPK signaling in placenta caused reduced expression of PPARγ, which affected GCM1 expression and probably contributed to the phenotype.

To extend our findings to additional potential target genes, we performed microarray experiments with RNA extracted from E12.5 wt, *Map2k1*$^{+/-}$ *Map2k2*$^{+/-}$ and *Map2k1*$^{flox/-}$ *Map2k2*$^{+/-}$ *Tg*$^{+/Sox2Cre}$ placentas. Venn diagrams (Fig. 7A) displaying the total number of transcripts up- and downregulated (P<0.05) reveal that the number of transcripts differentially expressed between *Map2k1*$^{flox/-}$ *Map2k2*$^{+/-}$ *Tg*$^{+/Sox2Cre}$ and wt was greater than that when the *Map2k1*$^{+/-}$ *Map2k2*$^{+/-}$ and wt groups were compared. Moreover, most genes were more dysregulated in *Map2k1*$^{flox/-}$ *Map2k2*$^{+/-}$ *Tg*$^{+/Sox2Cre}$ specimens than in *Map2k1*$^{+/-}$ *Map2k2*$^{+/-}$ placentas. *Map2k1* and *Map2k2* transcripts were downregulated in both *Map2k1*$^{+/-}$ *Map2k2*$^{+/-}$ and *Map2k1*$^{flox/-}$ *Map2k2*$^{+/-}$ *Tg*$^{+/Sox2Cre}$ groups, validating the experimental approach (Fig. 7C; not shown). Thus, the lack of an additional *Map2k1* allele in

Development (2014) 141, 2825-2837 doi:10.1242/dev.107409

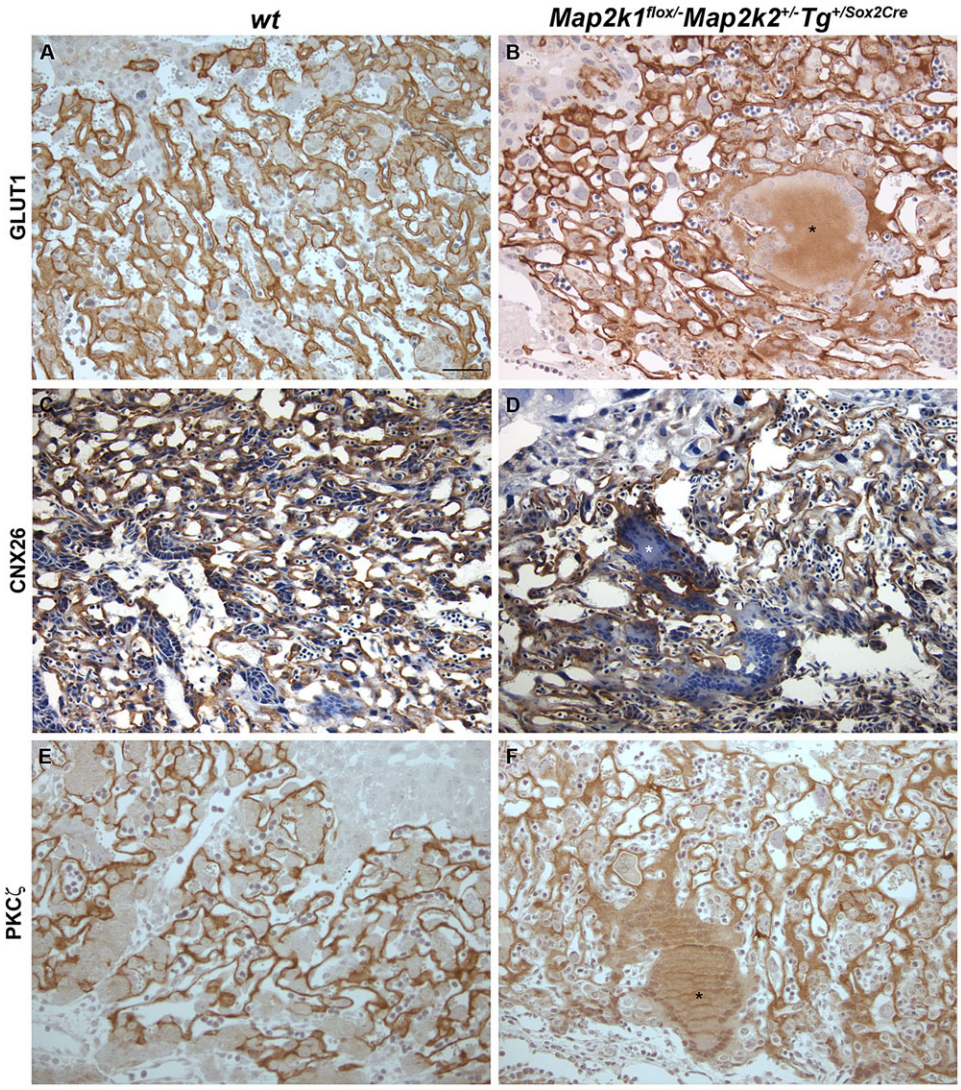

Fig. 4. Protein mislocalization in MTGs. GLUT1 (A,B), connexin 26 (C,D) and PKCζ (E,F) immunostainings were performed on placenta from E12.5 wt (A,C,E) and *Map2k1*$^{flox/-}$ *Map2k2*$^{+/-}$ *Tg*$^{+/Sox2Cre}$ (B,D,F) embryos. GLUT1 staining was observed in SynT-I and SynT-II membranes of wt and *Map2k1*$^{flox/-}$ *Map2k2*$^{+/-}$ *Tg*$^{+/Sox2Cre}$ specimens. An abnormal cytoplasmic signal was also observed in MTGs (asterisk) and in adjacent cells (B). Connexin 26 signal was detected at the SynT membranes of wt and *Map2k1*$^{flox/-}$ *Map2k2*$^{+/-}$ *Tg*$^{+/Sox2Cre}$ specimens as well as in the membrane surrounding MTGs (D). PKCζ immunostaining was present at the SynT-I membrane in wt and *Map2k1*$^{flox/-}$ *Map2k2*$^{+/-}$ *Tg*$^{+/Sox2Cre}$ placentas (E,F). In MTGs, PKCζ was mislocalized in the cytoplasm (asterisk). Scale bar: 50 µm.

allantois-derived tissues in the *Map2k1*$^{+/-}$ *Map2k2*$^{+/-}$ background had a greater impact on the placenta transcriptome than the absence of one allele of each *Map2k1/2* gene, which correlated with the exacerbated phenotype of *Map2k1*$^{flox/-}$ *Map2k2*$^{+/-}$ *Tg*$^{+/Sox2Cre}$ specimens.

To identify the biological processes affected in mutant placentas, we used the DAVID functional annotation chart algorithm (Huang et al., 2009). Upregulated genes in *Map2k1*$^{flox/-}$ *Map2k2*$^{+/-}$ *Tg*$^{+/Sox2Cre}$ placentas were associated with processes involving organelle and protein localization, transport, metabolism and apoptosis, whereas downregulated genes were enriched in cell structure and mobility, DNA organization, placenta development, protein localization, regulation of signal transduction and organelle organization processes (P<0.01; Fig. 7B). In the *Map2k1*$^{+/-}$ *Map2k2*$^{+/-}$ group, fewer biological processes were enriched and fewer dysregulated genes were found in each affected process (not shown).

Several of the processes dysregulated in *Map2k1 Map2k2* mutants could contribute to the placenta phenotype. Our results indicated that genes associated with syncytiotrophoblast cell fusion or differentiation, such as *Syna*, *Synb*, caveolin 1, syntaxin 3 and axin1 upregulated gene (*Axud1*; also known as *Csrnp1*), were upregulated in mutant specimens (not shown) (Collett et al., 2010; Dupressoir et al., 2009, 2011; Ishiguro et al., 2001; Palfreyman and Jorgensen, 2009). By contrast, PKA catalytic unit β (*Prkacb*), which encodes a regulator of *Gcm1* expression, and *Cyr61*, which is involved in syncytiotrophoblast cell fusion, were downregulated (not shown) (Matsuura et al., 2011; Mo et al., 2002). Expression of *Slpi*, which encodes a secretory leukocyte protease inhibitor implicated in syncytiotrophoblast differentiation and fusion, was also repressed in mutant placentas, as confirmed by qRT-PCR (Fig. 7C) (Neelima and Rao, 2008). Thus, the concomitant upregulation and downregulation of genes promoting and repressing cell fusion, respectively, support the notion that SynT cell fusion defects participate in MTG formation.

The expression of *Cdx2*, *Esrrb* and *Tcfap2c*, which encode transcription factors important for trophoblast cell fate specification and differentiation, was also downregulated in mutants (Fig. 7C; not shown) (Kuckenberg et al., 2010; Luo et al., 1997; Strumpf et al., 2005). Immunofluorescence data confirmed the decreased CDX2 expression in mutants and also revealed that, throughout placenta development, CDX2-positive cells are detected at the chorio-allantoic interface, where SynT progenitors are proposed to be located (Fig. 7D) (Simmons et al., 2008).

Cdx2 has been shown to play a role in cell polarity by controlling protein trafficking allowing apical-basal transport (Gao and

Development (2014) 141, 2825-2837 doi:10.1242/dev.107409

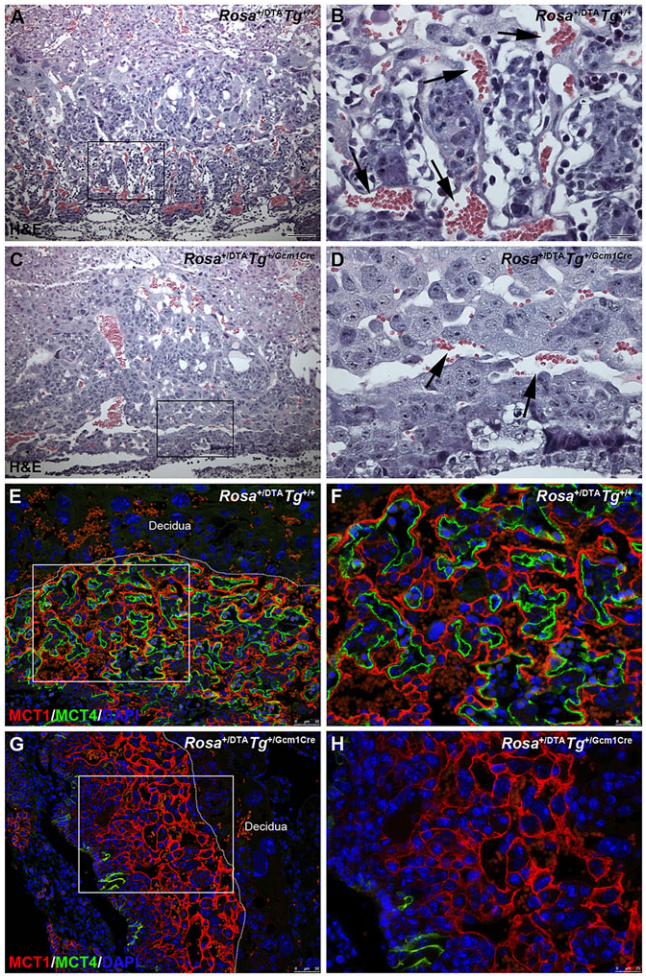

Fig. 5. The genetic ablation of SynT-II cells impacts on SynT-I cell fusion. *Rosa*$^{+/DTA}$ *Tg*$^{+/Gcm1Cre}$ embryos were produced to generate placenta without SynT-II. (A-D) H&E staining of placenta sections from E10.5 wt (A,B) and *Rosa*$^{+/DTA}$ *Tg*$^{+/Gcm1Cre}$ (C,D) embryos, showing that the labyrinth of the *Rosa*$^{+/DTA}$ *Tg*$^{+/Gcm1Cre}$ specimens was more compact with an absence of intermingling maternal sinuses and fetal blood vessels. Arrows (B,D) indicate maternal sinuses. (E-H) MCT1 and MCT4 IF was used to monitor SynT-I and -II cells, respectively, on placenta sections from E10.5 *Rosa*$^{+/DTA}$ *Tg*$^{+/+}$ and *Rosa*$^{+/DTA}$ *Tg*$^{+/Gcm1Cre}$ embryos. In control specimens, MCT1 and MCT4 staining was detected at the apical and basal membranes of SynT-I and -II, respectively (E,F). In *Rosa*$^{+/DTA}$ *Tg*$^{+/Gcm1Cre}$ placentas, only a few MCT4-positive cells were detected, revealing efficient ablation of the SynT-II cells, whereas the MCT1 signal was associated with mononucleated cells indicating the absence of syncytium formation (G,H). The boxed regions in A,C,E,G are magnified in B,D,F,H. Scale bars: 20 μm in B,D; 25 μm in F,H; 50 μm in E,G; 100 μm in A,C.

Kaestner, 2010). Microarray and IHC analyses showed that expression and localization of the SynT polarized proteins GLUT1, MCT1 and PKCζ were affected in mutants (Figs 3, 4) (Nagai et al., 2010; Shalom-Barak et al., 2004). Moreover, *Muc1*, a transcriptional PPARγ target that encodes a mucin present at the apical membrane of SynT-I, was downregulated in *Map2k1*$^{flox/-}$ *Map2k2*$^{+/-}$ *Tg*$^{+/Sox2Cre}$ mutants (Fig. 7C). Lastly, genes involved in epithelial cell polarity, such as *Prkcz*, which encodes the PKCζ protein, and members of the Hippo signaling pathway, such as *Frmd6*, *Rassf1/4/5* and *Yap1*, were dysregulated in mutants (Fig. 7C) (Genevet and Tapon, 2011). Expression of the transcription factor YAP1 was increased in MTG nuclei. Moreover, an accumulation of the phosphorylated, inactivated form of YAP1, was detected in MTG cytoplasm, reinforcing the notion that cell polarity is defective in *Map2k1 Map2k2* mutants (Fig. 7E). Thus, the combined mutations of *Map2k1* and *Map2k2* in placenta affect the expression of numerous genes involved in cell fate specification, cell fusion and cell polarity, and this is likely to explain the underdeveloped placenta and the MTG phenotype seen in *Map2k1 Map2k2* mutants.

DISCUSSION

Our previous studies revealed that the loss of *Map2k1* function leads to placental defects characterized by a reduced labyrinth region and maternal and embryonic hypovascularization (Giroux et al., 1999). Proliferation and survival of the labyrinth trophoblasts are reduced in *Map2k1*$^{-/-}$ placenta. SynT-II cells are determined but they are blocked at the chorio-allantoic interface, being unable to invade the labyrinth region to initiate placental vascularization (Bissonauth et al., 2006). These data indicated that *Map2k1* is important for the proliferation and survival of labyrinth trophoblasts and that it may be required for SynT-II migration and terminal differentiation as processes crucial for the full expansion of the fetal-maternal exchange area. Here, we showed that the specific mutation of *Map2k1* in SynT-II in *Map2k1*$^{flox/-}$ *Tg*$^{+/Gcm1Cre}$ specimens did not affect placenta development or embryo survival. Thus, *Map2k1* function is not essential in SynT-II for the differentiation and migration of these cells. The incapacity of SynT-II cells to invade the labyrinth in *Map2k1*$^{-/-}$ placenta might be a consequence of the underdevelopment of the labyrinth.

The phenotype of *Map2k1*$^{+/-}$ *Map2k2*$^{+/-}$ embryos established that a critical dosage of *Map2k1* and *Map2k2* genes is required in the placenta to allow embryo development to proceed to term (Nadeau et al., 2009). Here, we showed that targeting the *Map2k1* deletion to specific cell types does not have the same consequences for placenta development. For instance, deletion of one *Map2k1* allele in SynT-II cells from *Map2k1*$^{+/flox}$ *Map2k2*$^{+/-}$ *Tg*$^{+/Gcm1Cre}$ embryos caused placenta defects at higher penetrance and expressivity than the inactivation of one *Map2k1* allele in allantoic-derived tissues in *Map2k1*$^{+/flox}$ *Map2k2*$^{+/-}$ *Tg*$^{+/Sox2Cre}$ embryos (Table 1). Thus, the requirement for the ERK/MAPK pathway is not equivalent in all cell types of the placenta.

The placenta phenotype of *Map2k1*$^{+/flox}$ *Map2k2*$^{+/-}$ *Tg*$^{+/Gcm1Cre}$ embryos was less severe than that of *Map2k1*$^{+/-}$ *Map2k2*$^{+/-}$ specimens, demonstrating that reduced expression levels of *Map2k1* and *Map2k2* in SynT-II cells are not sufficient to reproduce the *Map2k1*$^{+/-}$ *Map2k2*$^{+/-}$ placenta defects. An altered ERK/MAPK pathway in other placenta tissues is also required for the full expressivity of the phenotype. The deletion of both *Map2k1* alleles in allantois-derived tissues in *Map2k1*$^{flox/-}$ *Map2k2*$^{+/-}$ *Tg*$^{+/Sox2Cre}$ specimens amplified the MTG phenotype, demonstrating an essential role for MAP2K1 in the allantois for the proper differentiation and fusion of SynT cells. The MTG phenotype was also worsened in *Map2k1*$^{flox/-}$ *Tg*$^{+/Gcm1Cre}$ *Tg*$^{+/Sox2Cre}$ mutants when compared with *Map2k1*$^{flox/-}$ *Tg*$^{+/Gcm1Cre}$ specimens but was not as severe as the phenotype seen in *Map2k1*$^{+/-}$ *Map2k2*$^{+/-}$ mutants. Thus, reduced levels of both MAP2K1 and MAP2K2 proteins in SynT-II and in allantois-derived tissues are required for the full expressivity of the placenta phenotype.

The specific deletion of *Map2k1* function in pericytes of *Map2k1*$^{flox/-}$ *Map2k2*$^{+/-}$ *Dermo1*$^{+/Cre}$ specimens also affected placenta development. The phenotype was intermediate between those of *Map2k1*$^{+/-}$ *Map2k2*$^{+/-}$ and *Map2k1*$^{flox/-}$ *Map2k2*$^{+/-}$ *Tg*$^{+/Sox2Cre}$. This indicates that *Map2k1* function in pericytes contributes to placenta formation but that the ERK/MAPK pathway

Development (2014) 141, 2825-2837 doi:10.1242/dev.107409

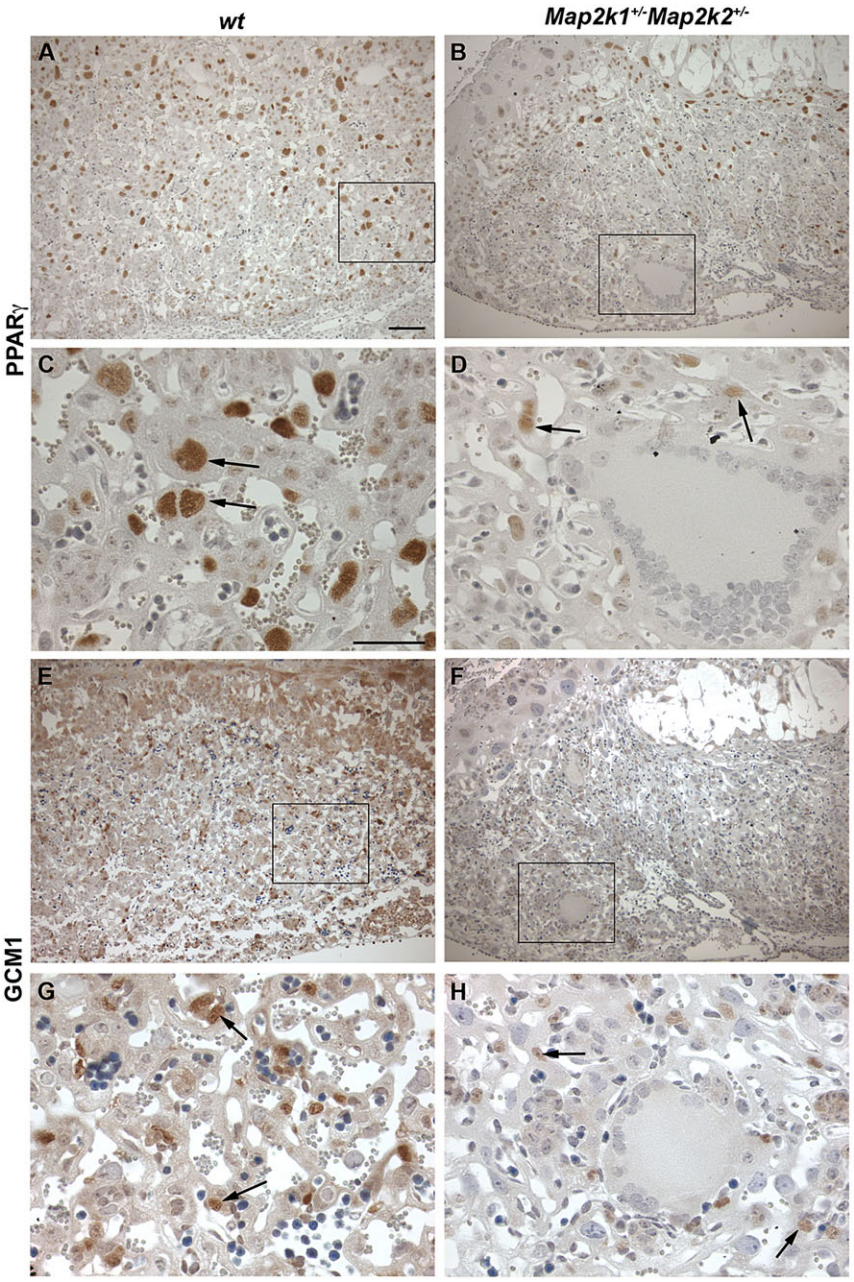

Fig. 6. Downregulation of PPARγ and GCM1 expression in *Map2k1*$^{+/-}$ *Map2k2*$^{+/-}$ placenta. (A-D) PPARγ expression was evaluated by IHC. In placenta from E12.5 wt embryos, PPARγ was detected in the nuclei of trophoblasts throughout the labyrinthine region (boxed area). In *Map2k1*$^{+/-}$ *Map2k2*$^{+/-}$ specimens, PPARγ expression was reduced in the labyrinth trophoblasts located near MTGs (arrows). No PPARγ signal was detected in MTG nuclei. (E-H) GCM1 expression at E12.5 was detected in SynT-II nuclei (arrows), although it was reduced in *Map2k1*$^{+/-}$ *Map2k2*$^{+/-}$ compared with wt. No signal was observed in MTG nuclei. The boxed regions in A,B,E,F are magnified in C,D,G,H. Scale bars: 50 µm in A,B,E,F; 100 µm in C,D,G,H.

in other allantois-derived cell types, most likely endothelial cells, also participates in placenta development. Pericytes are necessary for the maintenance of endothelial cell integrity (Armulik et al., 2005; Hellstrom et al., 2001). Therefore, the ERK/MAPK pathway might be required in pericytes to preserve endothelial cell functions, allowing adequate differentiation of SynT-II. In agreement with this, the *Map2k1* deletion in pericytes in a *Map2k2* null background (*Map2k1*$^{flox/flox}$ *Map2k2*$^{-/-}$ *Dermo1*$^{+/Cre}$) affected the vascularization of the labyrinth by endothelial cells, but not the migration of pericytes as observed by PECAM and αSMA immunostaining (not shown). Altogether, our results demonstrate that a functional ERK/MAPK pathway is necessary in SynT-II and allantois-derived tissues, including pericytes, to support the correct development of the placenta.

The non-cell-autonomous dependence on allantois derivatives for MTG formation has also been observed in other mutant mice, such as the *Lbp-1a* mutants (Parekh et al., 2004). LBP-1a is a target of the ERK/MAPK pathway. Phosphorylation of LBP-1 proteins by ERK potentiates their DNA binding capacity and their transcriptional activity (Pagon et al., 2003; Volker et al., 1997). It is conceivable that the reduced ERK signaling in the allantois can contribute to the MTG phenotype by affecting LBP-1a phosphorylation levels and its transcriptional activity. Thus, LBP-1 proteins might contribute to the production of signals by the allantois that are transduced by the ERK/MAPK pathway in SynT-II. Consequently, aberrant signaling between SynT and allantoic mesoderm perturbs placenta development. The ERK/MAPK pathway might therefore play a role in different cell types of the placenta to regulate the production of signals and their integration.

During mouse placenta development, each SynT layer is generated by cell-cell fusion to form the contiguous layers I and II. These layers remain distinct due to differentially expressed fusogenic proteins, such as syncytins A and B and their respective receptors, which are still unknown in mice (Dupressoir et al., 2009, 2011; Simmons et al., 2008). Interactions between both layers appear essential for the formation of

Development (2014) 141, 2825-2837 doi:10.1242/dev.107409

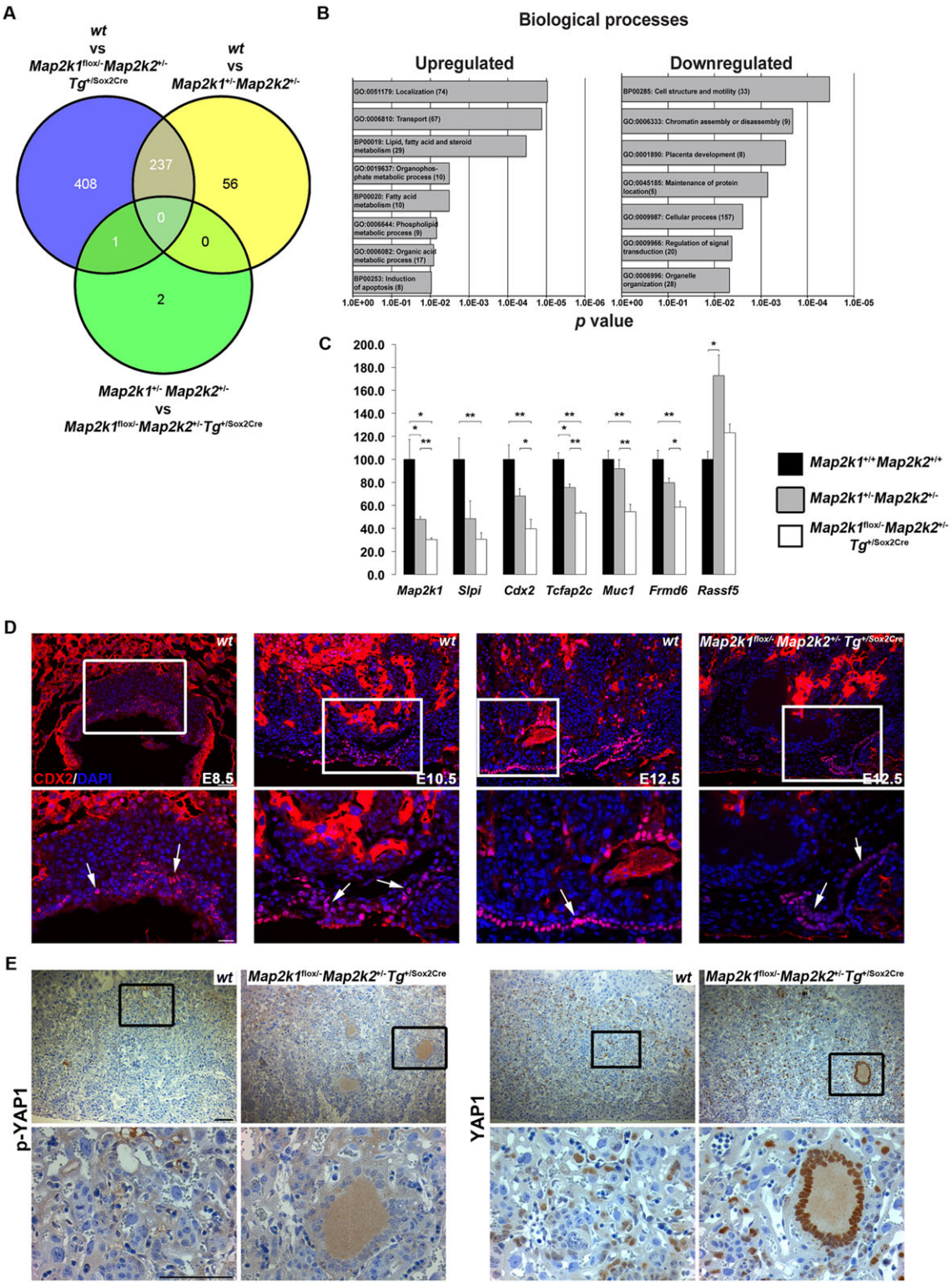

Fig. 7. Differential gene expression in placenta from E12.5 *Map2k1*$^{+/-}$ *Map2k2*$^{+/-}$ and *Map2k1*$^{flox/-}$ *Map2k2*$^{+/-}$ *Tg*$^{+/Sox2Cre}$ embryos. (A) Venn diagrams illustrating the overlap of genes that are statistically differentially expressed (Benjamini Hochberg adjusted $P<0.05$) between genotypes. (B) Gene ontology enrichment analysis of over-represented biological processes for genes up- and downregulated in placenta from E12.5 *Map2k1*$^{+/-}$ *Map2k2*$^{+/-}$ and *Map2k1*$^{flox/-}$ *Map2k2*$^{+/-}$ *Tg*$^{+/Sox2Cre}$ embryos relative to wt specimens. Biological process enrichment was calculated from the microarray data using the DAVID web portal, which calculates a *P*-value based on the probability that a process appears in the dataset relative to that expected by random chance. All the enriched terms have $P<0.01$. (C) qRT-PCR analyses for *Map2k1*, *Slpi*, *Cdx2*, *Tcfap2c*, *Muc1*, *Frmd6* and *Rassf5* confirmed the microarray data. Values are mean±s.e.m. (n=4-8 per group) of expression relative to wt (100%); $P<0.05$, $^{**}P<0.01$. (D) CDX2 immunostaining revealed a population of CDX2-positive cells at the chorio-allantoic interface as early as E8.5 (arrows). Reduced CDX2 expression was detected in E12.5 *Map2k1*$^{flox/-}$ *Map2k2*$^{+/-}$ *Tg*$^{+/Sox2Cre}$ specimens. (E) Immunostainings revealed the presence of phospho-YAP1 in MTG cytoplasm, whereas YAP1 was highly expressed in MTG nuclei. (D,E) Boxed regions are magnified beneath. Scale bars: 25 µm in D, lower panels; 50 µm in D, upper panels; 100 µm in E.

Development (2014) 141, 2825-2837 doi:10.1242/dev.107409

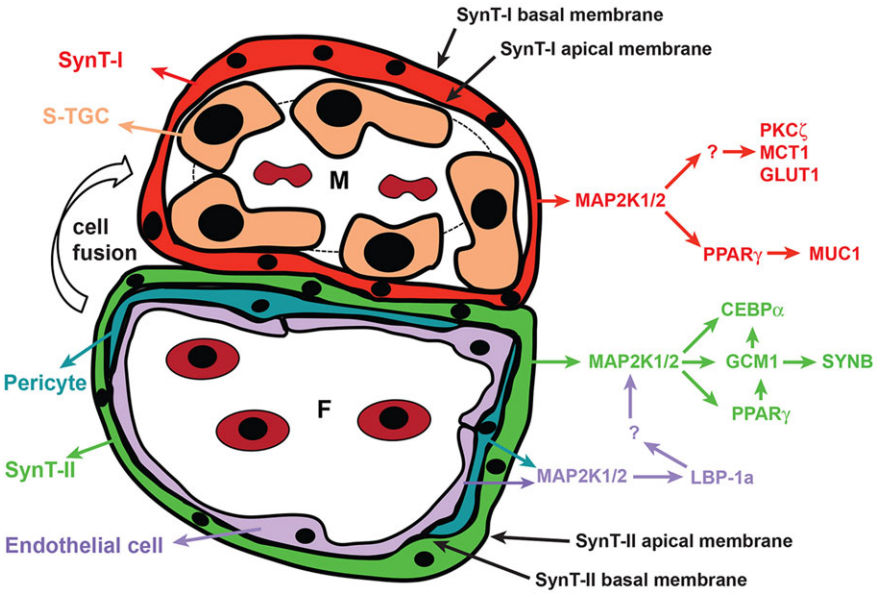

Fig. 8. Model for the role of the ERK/MAPK pathway in blood-placental barrier formation. In the SynT-I surrounding the maternal blood sinuses, the ERK/MAPK pathway controls the expression and activity of PPARγ, a direct regulator of *Muc1*, and the cellular distribution of GLUT1, MCT1 and PKCζ. In the SynT-II encircling the fetal blood vessels, the ERK/MAPK cascade acts on several players, including GCM1, CEBPα and PPARγ, a direct regulator of *Gcm1*. The GCM1 transcription factor regulates the expression of *Synb* and *Cebpa*. In pericytes and endothelial cells, which both derive from the allantois, we propose that the ERK/MAPK pathway might be involved in the regulation of the activity of LBP-1a (UBP1), which is known to contribute to SynT cell differentiation. The SynT-II layer is essential for SynT-I cell fusion. Improper ERK/MAPK signaling perturbs SynT-II differentiation and SynT-I–SynT-II interactions, which leads to MTG development. M, maternal blood sinus; F, fetal blood vessel.

the placenta, since the specific ablation of SynT-II cells in embryos disrupted SynT-I cell fusion and subsequent placenta formation. These results confirmed electron microscopy observations showing that the fusion of SynT-I cells occurs solely after contacts with SynT-II (Hernandez-Verdun, 1974). The ablation of SynT-II cells also affected maternal vascularization, which supports the concept that the formation of the SynT-II syncytium is required for interactions with neighboring trophoblasts (Dupressoir et al., 2011). Interestingly, the determination of SynT-I does not require the presence of SynT-II, since MCT1-positive cells were observed in the absence of SynT-II in *Rosa*$^{+/DTA}$ *Tg*$^{+/Gcm1Cre}$ mutants. Therefore, SynT-II is essential for SynT-I cell fusion but not for SynT-I cell fate determination.

The origin of MTGs is intriguing. In *Map2k1 Map2k2* mutants, MTGs expressed markers of both SynT layers, suggesting that they could originate from cell fusion between SynT layers. MTGs expressed MCT1, *Syna*, PAX8 and PKCζ, which are specific markers of SynT-I, and also MCT4, a SynT-II marker. Surprisingly, even though MTGs have been shown to derive from SynT-II cells, the expression of transcription factors involved in SynT-II cell determination and differentiation, such as GCM1 and its transcriptional targets *Cebpa* and *Synb*, was not detected in MTGs (Nadeau et al., 2009; Simmons et al., 2008). This result is in agreement with previous reports showing that the ERK/MAPK pathway and its target PPARγ are involved in *Gcm1* expression (Fernandez-Serra et al., 2004; Burgermeister et al., 2007; Camp and Tafuri, 1997; Parast et al., 2009; Prusty et al., 2002). The decreased ERK/MAPK activation seen in *Map2k1 Map2k2* mutants thus leads to reduced PPARγ and consequently to the loss of GCM1 expression. This might explain the decrease in *Cebpa* and *Synb* expression resulting in the absence of SynT-II-specific markers (Fig. 8). Altogether, our results suggest that MTGs derive from aberrant fusion between SynT-I and SynT-II cells. Unfortunately, we cannot assess the contribution of SynT-I cells to the formation of MTGs, as has been done previously for SynT-II cells, as it would require cell lineage experiments with a SynT-I-specific *Cre* deleter mouse line, which is not available (Nadeau et al., 2009). Therefore, we cannot rule out the possibility that reduced ERK/MAPK signaling leads to the transdifferentiation of SynT-II into SynT-I cells.

SynT differentiation implies the specific localization of polarized proteins that allow the SynT-I and -II cells to accomplish their function in an exchange epithelium. The apical and basolateral membrane domains of epithelial cells are usually defined by the antagonistic action of protein complexes located in the apical-basolateral membrane junction (Muller and Bossinger, 2003; Tepass et al., 2001). Overexpression of mouse atypical PKCζ was shown to cause expansion of the apical cell membrane in frog blastomeres, which become rounded with protrusions, demonstrating that PKCζ is necessary for apical membrane identity (Chalmers et al., 2005). Here, we showed that PKCζ is specifically expressed at the apical membrane of SynT-I in wt specimens. In *Map2k1 Map2k2* mutants, PKCζ expression was increased and accumulated in MTG cytoplasm. Apical proteins, such as MCT1 and GLUT1, were also mislocalized. Our results thus establish that there are critical cell polarity defects in these mutants.

The Hippo signaling pathway is involved in the regulation of cell polarity. In the absence of Hippo signaling, YAP1 is not phosphorylated and is translocated to the nucleus, where it participates in the expansion of the apical domain (Genevet et al., 2009; Hamaratoglu et al., 2009). In *Drosophila*, misexpression of regulators of cell polarity, such as LGL, atypical PKC and Crumbs, was shown to control the Hippo pathway by affecting the localization of Hippo, Rassf and Expanded (Grzeschik et al., 2010). In *Map2k1 Map2k2* mouse mutants, *Yap1* upregulation correlated with the accumulation of nuclear YAP1 and cytoplasmic phospho-YAP1 in MTGs. Furthermore, regulators of the Hippo pathway were overexpressed (*Rassf5*, *Frmd6*) or downregulated (*Rassf1*/*4*), suggesting that the Hippo pathway is dysregulated in *Map2k1 Map2k2* placenta. The perturbed Hippo pathway thus offers a mechanistic explanation for the abnormal cell polarity in MTGs.

Microarray data revealed the upregulation of several membrane transporters in *Map2k1 Map2k2* mutant placentas, which might reflect compensatory mechanisms for the reduced placenta vascularization in order to maintain maternal-fetal exchanges. However, these mechanisms appeared to be insufficient for embryo survival. In human, the sodium-dependent neutral amino acid transporter type 2 (ASCT2; also known as SLC1A5) and the major facilitator superfamily transporter MFSD2A are the genuine receptors of syncytin 1 and 2 (ERVW-1 and ERVFRD-1), respectively (Cheynet et al., 2006; Esnault et al., 2008). In mice, the syncytin A

Development (2014) 141, 2825-2837 doi:10.1242/dev.107409

and B receptors are undefined, but we can hypothesize that, as in human, they would correspond to transporters upregulated in *Map2k1 Map2k2* mutant specimens. Their ectopic expression in inappropriate cell types could lead to cell fusion between SynT-I and -II and cause the dual identity of MTGs.

It has been proposed that the postmitotic SynT-I and SynT-II cells originate from distinct precursor populations expressing layer-specific gene markers as early as E8.5 (Cross et al., 2006; Simmons et al., 2008). SynT-II progenitors are suspected to be small, compact, cuboidal cells located at the interface between the chorionic ectoderm and the allantoic mesoderm. They represent a pool of fusion-competent cells that are still proliferating and persist until mid-gestation. We showed that a single layer of cuboidal cells located at the interface of the chorionic ectoderm and allantoic mesoderm expressed CDX2 at E8.5, suggesting that these cells correspond to SynT-II progenitors. CDX2 is a transcription factor essential for the specification of trophoblast stem (TS) cells (Rossant and Cross, 2001; Takao et al., 2012). TS cell maintenance in the early embryo depends on FGF4 signaling that controls *Cdx2* expression (Murohashi et al., 2010; Takao et al., 2012). In *Map2k1 Map2k2* mutants, *Cdx2* expression was reduced, which might contribute to the labyrinth growth defect. Thus, the ERK/MAPK pathway might be involved in the control of *Cdx2* expression via FGF signaling and in the proliferation of the progenitors that sustain the growth of the labyrinth and the production of SynT-II. Data from our microarray analysis further support the importance of the ERK/MAPK pathway in labyrinth trophoblasts. Decreased expression of *Mash2* (*Ascl2*), which co-localizes with *Cdx2* in mouse labyrinth, was observed in *Map2k1 Map2k2* mutants (not shown; Takao et al., 2012). MASH2 is expressed in trophoblast progenitors. Its knockdown in TS cells represses *Gcm1* expression while increasing expression of placental lactogen 1 (*Pl1*; also known as *Prl3d1*), a trophoblast giant cell marker, suggesting that it can participate in SynT-II specification (Takao et al., 2012). The expression of *Tcfap2c* and *Esrrb*, which are also involved in TS cell maintenance, was diminished in *Map2k1 Map2k2* mutant placenta (Kuckenberg et al., 2010; Luo et al., 1997). Finally, PPARγ, which was downregulated in *Map2k1 Map2k2* mutants, was shown to be necessary for TS cell maintenance and for subsequent SynT differentiation, reinforcing the idea that ERK/MAPK activation is crucial for labyrinth trophoblast differentiation (Parast et al., 2009).

In summary, normal levels of ERK/MAPK signaling in cell types of different embryonic and extraembryonic origins are required for the formation of the SynT-I and -II layers. This unique maternal-fetal exchange epithelia that form the blood-placental barrier are crucial for embryo development. The ERK/MAPK pathway also contributes to cell polarity, cell growth and differentiation of SynT and to syncytium formation. Our studies also significantly advance our understanding of labyrinth formation through the identification of new markers for SynT-I (PAX8 and PKCζ), as well as demonstrating for the first time the requirement of SynT-II for the formation of the SynT-I syncytium.

MATERIALS AND METHODS

Mice, genotyping and tissue collection

The Map2k1$^{flox/flox}$, Map2k2$^{-/-}$ and *Gcm1Cre* mouse lines were described previously (Bélanger et al., 2003; Bissonauth et al., 2006; Nadeau et al., 2009). Four *Gcm1Cre* transgenic lines were obtained with a 185 kb *Gcm1Cre* BAC transgene, which was imprinted in all four lines. Only the paternal allele was expressed and it was active in germ cells. To circumvent this limitation, we used *Map2k1*$^{+/-}$ *Tg*$^{+/Gcm1Cre}$ males to generate experimental specimens. The *Gcm1Cre* 185kb-2 line, named hereafter *Gcm1Cre*, was utilized (supplementary material Fig. S1). The *Gt(ROSA)26Sor*^{tm1Sor} (*Rosa*^{lacZ}), *Gt(ROSA)26Sor*$^{tm4(ACTB-tdTomato-EGFP)Luo}$ (*Rosa*$^{Tomato-EGFP}$) and *Gt(ROSA)26Sor*$^{tm1(DTA)Jpmb}$ (*Rosa*^{DTA}) mouse lines were purchased at the Jackson Laboratory (Ivanova et al., 2005; Muzumdar et al., 2007; Soriano, 1999). The *Sox2Cre* and *Dermo1Cre* mouse lines were obtained from Dr A. McMahon and Dr D. Ornitz, respectively (Hayashi et al., 2002; Yu et al., 2003). The specificity of Cre-mediated recombination was validated (supplementary material Fig. S1). Experimental specimens were genotyped by Southern blot and PCR analyses. Placentas from control and mutant embryos were collected at E10.5 and E12.5. For RNA extraction, placentas were snap-frozen in liquid nitrogen. Experiments were performed according to the guidelines of the Canadian Council on Animal Care and were approved by the institutional animal care committee.

Histological, immunohistochemical (IHC) and immunofluorescence (IF) analyses

Specimens were collected and processed for paraffin (4 µm) or frozen (6 µm) sections as described (Bissonauth et al., 2006). Sagittal placenta sections were stained with Hematoxylin and Eosin (H&E) and Oil Red O according to standard histological procedures. The placenta was oriented with the maternal side at the top and the fetal (flat) side at the bottom. The plane of sectioning was through the center of the placenta and perpendicular to its flat surface. The number and the area of MTGs in the section were calculated every 25 sections (~100 µm apart) on four sections for each specimen. Primary and secondary antibodies for IHC and IF experiments are listed in supplementary material Table S1. IHC experiments were performed as previously described (Nadeau et al., 2009). Horseradish peroxidase activity was detected with the diaminobenzidine reagent kit (Zymed Laboratories) or the tyramide signal amplification (TSA) system (PerkinElmer). For co-IF analyses, primary antibodies were added simultaneously and nuclei were visualized by DAPI staining. At least three specimens per genotype were tested and representative fields are presented.

In situ hybridization (ISH) and β-galactosidase staining

Radioactive ISH was performed on tissue sections with *Gcm1*, *Syna* and *Synb* riboprobes. β-galactosidase staining was performed on cryosections as described (Nadeau et al., 2009).

RNA isolation, microarray analysis and quantitative RT-PCR (qRT-PCR)

Placentas from E12.5 wt, *Map2k1*$^{+/-}$ *Map2k2*$^{+/-}$ and *Map2k1*$^{flox/-}$ *Map2k2*$^{+/-}$ *Tg*$^{+/Sox2Cre}$ embryos (n=4 per genotype) were collected. Placenta was dissected and half of the tissue was processed for histology to confirm the absence of maternal tissues. Total RNA was isolated from the second half using TRIzol reagent according to the manufacturer's procedure (Invitrogen). RNA quality and quantity assessment, cDNA probe preparation, hybridization to the Illumina Mouse WG-6 v2.0 Expression Beadchip, and image scans were performed at the Genome Quebec Innovation Centre at McGill University (Montreal, Canada). Data were normalized using $\log_2$ transformation followed by quantile normalization with the R/lumi package in BioConductor (Du et al., 2008). Raw and normalized data are available at the NCBI Gene Expression Omnibus database (http://www.ncbi.nlm.nih.gov/projects/geo) under accession number GSE51644 according to MIAME standards (Edgar et al., 2002). Significantly modulated probes were identified using the empirical Bayes statistics available in limma (Wettenhall and Smyth, 2004). Probes were considered significantly modulated when the Benjamini Hochberg adjusted P-value was less than 0.05.

qRT-PCR experiments were performed as described (Boucherat et al., 2012). Four specimens were used for each genotype tested. Primer sequences are listed in supplementary material Table S2.

Statistical analyses

Student's t-test was performed for comparative studies. $P<0.05$ was considered statistically significant.

Acknowledgements
We thank Drs Lucie Jeannotte, Steve Bilodeau and Rhea Utley for critical comments, Drs Andy McMahon, David Ornitz, Luc Bélanger and Jay Cross for reagents, Carl St-Pierre for technical assistance at the confocal microscope and Eric Paquet for help with the analysis of microarray data.

Competing interests
The authors declare no competing financial interests.

Author contributions
V.N. and J.C. designed the project, analyzed data and wrote the paper. V.N. performed the experiments.

Funding
This work was supported by the Canadian Institutes of Health Research (CIHR) [MOP-97801 to J.C.].

Supplementary material
Supplementary material available online at
http://dev.biologists.org/lookup/suppl/doi:10.1242/dev.107409/-/DC1

References

Anson-Cartwright, L., Dawson, K., Holmyard, D., Fisher, S. J., Lazzarini, R. A. and Cross, J. C. (2000). The glial cells missing-1 protein is essential for branching morphogenesis in the chorioallantoic placenta. *Nat. Genet.* **25**, 311-314.
Armulik, A., Abramsson, A. and Betsholtz, C. (2005). Endothelial/pericyte interactions. *Circ. Res.* **97**, 512-523.
Barak, Y., Nelson, M. C., Ong, E. S., Jones, Y. Z., Ruiz-Lozano, P., Chien, K. R., Koder, A. and Evans, R. M. (1999). PPAR gamma is required for placental, cardiac, and adipose tissue development. *Mol. Cell* **4**, 585-595.
Bélanger, L.-F., Roy, S., Tremblay, M., Brott, B., Steff, A.-M., Mourad, W., Hugo, P., Erikson, R. and Charron, J. (2003). Mek2 is dispensable for mouse growth and development. *Mol. Cell. Biol.* **23**, 4778-4787.
Bissonauth, V., Roy, S., Gravel, M., Guillemette, S. and Charron, J. (2006). Requirement for Map2k1 (Mek1) in extra-embryonic ectoderm during placentogenesis. *Development* **133**, 3429-3440.
Boucherat, O., Chakir, J. and Jeannotte, L. (2012). The loss of Hoxa5 function promotes Notch-dependent goblet cell metaplasia in lung airways. *Biol. Open* **1**, 677-691.
Burgermeister, E., Chuderland, D., Hanoch, T., Meyer, M., Liscovitch, M. and Seger, R. (2007). Interaction with MEK causes nuclear export and downregulation of peroxisome proliferator-activated receptor gamma. *Mol. Cell. Biol.* **27**, 803-817.
Camp, H. S. and Tafuri, S. R. (1997). Regulation of peroxisome proliferator-activated receptor gamma activity by mitogen-activated protein kinase. *J. Biol. Chem.* **272**, 10811-10816.
Chalmers, A. D., Pambos, M., Mason, J., Lang, S., Wylie, C. and Papalopulu, N. (2005). aPKC, Crumbs3 and Lgl2 control apicobasal polarity in early vertebrate development. *Development* **132**, 977-986.
Chang, C.-W., Chuang, H.-C., Yu, C., Yao, T.-P. and Chen, H. (2005). Stimulation of GCMa transcriptional activity by cyclic AMP/protein kinase A signaling is attributed to CBP-mediated acetylation of GCMa. *Mol. Cell. Biol.* **25**, 8401-8414.
Cheynet, V., Oriol, G. and Mallet, F. (2006). Identification of the hASCT2-binding domain of the Env ERVWE1/syncytin-1 fusogenic glycoprotein. *Retrovirology* **3**, 41.
Collett, G. P., Linton, E. A., Redman, C. W. G. and Sargent, I. L. (2010). Downregulation of caveolin-1 enhances fusion of human BeWo choriocarcinoma cells. *PLoS ONE* **5**, e10529.
Cross, J. C., Nakano, H., Natale, D. R. C., Simmons, D. G. and Watson, E. D. (2006). Branching morphogenesis during development of placental villi. *Differentiation* **74**, 393-401.
Du, P., Kibbe, W. A. and Lin, S. M. (2008). lumi: a pipeline for processing Illumina microarray. *Bioinformatics* **24**, 1547-1548.
Dupressoir, A., Marceau, G., Vernochet, C., Bénit, L., Kanellopoulos, C., Sapin, V. and Heidmann, T. (2005). Syncytin-A and syncytin-B, two fusogenic placenta-specific murine envelope genes of retroviral origin conserved in Muridae. *Proc. Natl. Acad. Sci. U.S.A.* **102**, 725-730.
Dupressoir, A., Vernochet, C., Bawa, O., Harper, F., Pierron, G., Opolon, P. and Heidmann, T. (2009). Syncytin-A knockout mice demonstrate the critical role in placentation of a fusogenic, endogenous retrovirus-derived, envelope gene. *Proc. Natl. Acad. Sci. U.S.A.* **106**, 12127-12132.
Dupressoir, A., Vernochet, C., Harper, F., Guegan, J., Dessen, P., Pierron, G. and Heidmann, T. (2011). A pair of co-opted retroviral envelope syncytin genes is required for formation of the two-layered murine placental syncytiotrophoblast. *Proc. Natl. Acad. Sci. U.S.A.* **108**, E1164-E1173.
Edgar, R., Domrachev, M. and Lash, A. E. (2002). Gene Expression Omnibus: NCBI gene expression and hybridization array data repository. *Nucleic Acids Res.* **30**, 207-210.
Esnault, C., Priet, S., Ribet, D., Vernochet, C., Bruls, T., Lavialle, C., Weissenbach, J. and Heidmann, T. (2008). A placenta-specific receptor for the fusogenic, endogenous retrovirus-derived, human syncytin-2. *Proc. Natl. Acad. Sci. U.S.A.* **105**, 17532-17537.
Fernandez-Serra, M., Consales, C., Livigni, A. and Arnone, M. I. (2004). Role of the ERK-mediated signaling pathway in mesenchyme formation and differentiation in the sea urchin embryo. *Dev. Biol.* **268**, 384-402.
Ferretti, E., Arturi, F., Mattei, T., Scipioni, A., Tell, G., Tosi, E., Presta, I., Morisi, R., Lacroix, L., Gulino, A. et al. (2005). Expression, regulation, and function of paired-box gene 8 in the human placenta and placental cancer cell lines. *Endocrinology* **146**, 4009-4015.
Galabova-Kovacs, G., Matzen, D., Piazzolla, D., Meissl, K., Plyushch, T., Chen, A. P., Silva, A. and Baccarini, M. (2006). Essential role of B-Raf in ERK activation during extraembryonic development. *Proc. Natl. Acad. Sci. U.S.A.* **103**, 1325-1330.
Gao, N. and Kaestner, K. H. (2010). Cdx2 regulates endo-lysosomal function and epithelial cell polarity. *Genes Dev.* **24**, 1295-1305.
Genevet, A. and Tapon, N. (2011). The Hippo pathway and apico-basal cell polarity. *Biochem. J.* **436**, 213-224.
Genevet, A., Polesello, C., Blight, K., Robertson, F., Collinson, L. M., Pichaud, F. and Tapon, N. (2009). The Hippo pathway regulates apical-domain size independently of its growth-control function. *J. Cell Sci.* **122**, 2360-2370.
Giroux, S., Tremblay, M., Bernard, D., Cadrin-Girard, J.-F., Aubry, S., Larouche, L., Rousseau, S., Huot, J., Landry, J., Jeannotte, L. et al. (1999). Embryonic death of Mek1-deficient mice reveals a role for this kinase in angiogenesis in the labyrinthine region of the placenta. *Curr. Biol.* **9**, 369-376.
Grzeschik, N. A., Parsons, L. M., Allott, M. L., Harvey, K. F. and Richardson, H. E. (2010). Lgl, aPKC, and Crumbs Regulate the Salvador/Warts/Hippo pathway through two distinct mechanisms. *Curr. Biol.* **20**, 573-581.
Hamaratoglu, F., Gajewski, K., Sansores-Garcia, L., Morrison, C., Tao, C. and Halder, G. (2009). The Hippo tumor-suppressor pathway regulates apical-domain size in parallel to tissue growth. *J. Cell Sci.* **122**, 2351-2359.
Hayashi, S., Lewis, P., Pevny, L. and McMahon, A. P. (2002). Efficient gene modulation in mouse epiblast using a Sox2Cre transgenic mouse strain. *Gene Expr. Patterns* **2**, 93-97.
Hellstrom, M., Gerhardt, H., Kalen, M., Li, X., Eriksson, U., Wolburg, H. and Betsholtz, C. (2001). Lack of pericytes leads to endothelial hyperplasia and abnormal vascular morphogenesis. *J. Cell Biol.* **153**, 543-554.
Hemberger, M. and Cross, J. C. (2001). Genes governing placental development. *Trends Endocrinol. Metab.* **12**, 162-168.
Hernandez-Verdun, D. (1974). Morphogenesis of the syncytium in the mouse placenta. Ultrastructural study. *Cell Tissue Res.* **148**, 381-396.
Huang, D. W., Sherman, B. T. and Lempicki, R. A. (2009). Systematic and integrative analysis of large gene lists using DAVID bioinformatics resources. *Nat. Protoc.* **4**, 44-57.
Ishiguro, H., Tsunoda, T., Tanaka, T., Fujii, Y., Nakamura, Y. and Furukawa, Y. (2001). Identification of AXUD1, a novel human gene induced by AXIN1 and its reduced expression in human carcinomas of the lung, liver, colon and kidney. *Oncogene* **20**, 5062-5066.
Ivanova, A., Signore, M., Caro, N., Greene, N. D. E., Copp, A. J. and Martinez-Barbera, J. P. (2005). In vivo genetic ablation by Cre-mediated expression of diphtheria toxin fragment A. *Genesis* **43**, 129-135.
Kubota, N., Terauchi, Y., Miki, H., Tamemoto, H., Yamauchi, T., Komeda, K., Satoh, S., Nakano, R., Ishii, C., Sugiyama, T. et al. (1999). PPAR gamma mediates high-fat diet-induced adipocyte hypertrophy and insulin resistance. *Mol. Cell* **4**, 597-609.
Kuckenberg, P., Buhl, S., Woynecki, T., van Furden, B., Tolkunova, E., Seiffe, F., Moser, M., Tomilin, A., Winterhager, E. and Schorle, H. (2010). The transcription factor TCFAP2C/AP-2gamma cooperates with CDX2 to maintain trophectoderm formation. *Mol. Cell. Biol.* **30**, 3310-3320.
Luo, J., Sladek, R., Bader, J.-A., Matthyssen, A., Rossant, J. and Giguère, V. (1997). Placental abnormalities in mouse embryos lacking the orphan nuclear receptor ERR-beta. *Nature* **388**, 778-782.
Matsuura, K., Jigami, T., Taniue, K., Morishita, Y., Adachi, S., Senda, T., Nonaka, A., Aburatani, H., Nakamura, T. and Akiyama, T. (2011). Identification of a link between Wnt/beta-catenin signalling and the cell fusion pathway. *Nat. Commun.* **2**, 548.
McCaffrey, L. M. and Macara, I. G. (2009). Widely conserved signaling pathways in the establishment of cell polarity. *Cold Spring Harb. Perspect. Biol.* **1**, a001370.
Mo, F.-E., Muntean, A. G., Chen, C.-C., Stolz, D. B., Watkins, S. C. and Lau, L. F. (2002). CYR61 (CCN1) is essential for placental development and vascular integrity. *Mol. Cell. Biol.* **22**, 8709-8720.
Müller, H.-A. and Bossinger, O. (2003). Molecular networks controlling epithelial cell polarity in development. *Mech. Dev.* **120**, 1231-1256.
Murohashi, M., Nakamura, T., Tanaka, S., Ichise, T., Yoshida, N., Yamamoto, T., Shibuya, M., Schlessinger, J. and Gotoh, N. (2010). An FGF4-FRS2alpha-Cdx2 axis in trophoblast stem cells induces Bmp4 to regulate proper growth of early mouse embryos. *Stem Cells* **28**, 113-121.
Muzumdar, M. D., Tasic, B., Miyamichi, K., Li, L. and Luo, L. (2007). A global double-fluorescent Cre reporter mouse. *Genesis* **45**, 593-605.

Development (2014) 141, 2825-2837 doi:10.1242/dev.107409

Nadeau, V., Guillemette, S., Belanger, L.-F., Jacob, O., Roy, S. and Charron, J. (2009). Map2k1 and Map2k2 genes contribute to the normal development of syncytiotrophoblasts during placentation. *Development* **136**, 1363-1374.

Nagai, A., Takebe, K., Nio-Kobayashi, J., Takahashi-Iwanaga, H. and Iwanaga, T. (2010). Cellular expression of the monocarboxylate transporter (MCT) family in the placenta of mice. *Placenta* **31**, 126-133.

Neelima, P. S. and Rao, A. J. (2008). Gene expression profiling during Forskolin induced differentiation of BeWo cells by differential display RT-PCR. *Mol. Cell. Endocrinol.* **281**, 37-46.

Ohno, M., Zannini, M., Levy, O., Carrasco, N. and di Lauro, R. (1999). The paired-domain transcription factor Pax8 binds to the upstream enhancer of the rat sodium/iodide symporter gene and participates in both thyroid-specific and cyclic-AMP-dependent transcription. *Mol. Cell. Biol.* **19**, 2051-2060.

Pagon, Z., Volker, J., Cooper, G. M. and Hansen, U. (2003). Mammalian transcription factor LSF is a target of ERK signaling. *J. Cell. Biochem.* **89**, 733-746.

Palfreyman, M. T. and Jorgensen, E. M. (2009). *In Vivo Analysis of Membrane Fusion*. Chichester: John Wiley & Sons.

Parast, M. M., Yu, H., Ciric, A., Salata, M. W., Davis, V. and Milstone, D. S. (2009). PPARgamma regulates trophoblast proliferation and promotes labyrinthine trilineage differentiation. *PLoS ONE* **4**, e8055.

Parekh, V., McEwen, A., Barbour, V., Takahashi, Y., Rehg, J. E., Jane, S. M. and Cunningham, J. M. (2004). Defective extraembryonic angiogenesis in mice lacking LBP-1a, a member of the grainyhead family of transcription factors. *Mol. Cell. Biol.* **24**, 7113-7129.

Prusty, D., Park, B.-H., Davis, K. E. and Farmer, S. R. (2002). Activation of MEK/ERK signaling promotes adipogenesis by enhancing peroxisome proliferator-activated receptor gamma (PPAR gamma) and C/EBP alpha gene expression during the differentiation of 3T3-L1 preadipocytes. *J. Biol. Chem.* **277**, 46226-46232.

Qian, X., Esteban, L., Vass, W. C., Upadhyaya, C., Papageorge, A., Yienger, K., Ward, J. M., Lowy, D. R. and Santos, E. (2000). The Sos1 and Sos2 Ras-specific exchange factors: differences in placental expression and signaling properties. *EMBO J.* **19**, 642-654.

Rossant, J. and Cross, J. (2001). Placental development: lessons from mouse mutants. *Nat. Rev. Genet.* **2**, 538-548.

Shalom-Barak, T., Nicholas, J. M., Wang, Y., Zhang, X., Ong, E. S., Young, T. H., Gendler, S. J., Evans, R. M. and Barak, Y. (2004). Peroxisome proliferator-activated receptor gamma controls Muc1 transcription in trophoblasts. *Mol. Cell. Biol.* **24**, 10661-10669.

Shin, B.-C., Suzuki, T., Matsuzaki, T., Tanaka, S., Kuraoka, A., Shibata, Y. and Takata, K. (1996). Immunolocalization of GLUT1 and connexin 26 in the rat placenta. *Cell Tissue Res.* **285**, 83-89.

Shin, B.-C., Fujikura, K., Suzuki, T., Tanaka, S. and Takata, K. (1997). Glucose transporter GLUT3 in the rat placental barrier: a possible machinery for the transplacental transfer of glucose. *Endocrinology* **138**, 3997-4004.

Simmons, D. G., Natale, D. R. C., Begay, V., Hughes, M., Leutz, A. and Cross, J. C. (2008). Early patterning of the chorion leads to the trilaminar trophoblast cell structure in the placental labyrinth. *Development* **135**, 2083-2091.

Soriano, P. (1999). Generalized lacZ expression with the ROSA26 Cre reporter strain. *Nat. Genet.* **21**, 70-71.

Sripathy, S., Lee, M. and Vasioukhin, V. (2011). Mammalian Llgl2 is necessary for proper branching morphogenesis during placental development. *Mol. Cell. Biol.* **31**, 2920-2933.

Strumpf, D., Mao, C.-A., Yamanaka, Y., Ralston, A., Chawengsaksophak, K., Beck, F. and Rossant, J. (2005). Cdx2 is required for correct cell fate specification and differentiation of trophectoderm in the mouse blastocyst. *Development* **132**, 2093-2102.

Takao, T., Asanoma, K., Tsunematsu, R., Kato, K. and Wake, N. (2012). The maternally expressed gene Tssc3 regulates the expression of MASH2 transcription factor in mouse trophoblast stem cells through the AKT-Sp1 signaling pathway. *J. Biol. Chem.* **287**, 42685-42694.

Tepass, U., Tanentzapf, G., Ward, R. and Fehon, R. (2001). Epithelial cell polarity and cell junctions in Drosophila. *Annu. Rev. Genet.* **35**, 747-784.

Volker, J. L., Rameh, L. E., Zhu, Q., DeCaprio, J. and Hansen, U. (1997). Mitogenic stimulation of resting T cells causes rapid phosphorylation of the transcription factor LSF and increased DNA-binding activity. *Genes Dev.* **11**, 1435-1446.

Wettenhall, J. M. and Smyth, G. K. (2004). limmaGUI: a graphical user interface for linear modeling of microarray data. *Bioinformatics* **20**, 3705-3706.

Wice, B., Menton, D., Geuze, H. and Schwartz, A. L. (1990). Modulators of cyclic AMP metabolism induce syncytiotrophoblast formation in vitro. *Exp. Cell Res.* **186**, 306-316.

Yu, K., Xu, J., Liu, Z., Sosic, D., Shao, J., Olson, E. N., Towler, D. A. and Ornitz, D. M. (2003). Conditional inactivation of FGF receptor 2 reveals an essential role for FGF signaling in the regulation of osteoblast function and bone growth. *Development* **130**, 3063-3074.